Moderately degenerated human intervertebral discs exhibit a less geometrically specific collagen fiber orientation distribution

Roman Dittmar[1*], Marc M. van Rijsbergen[1*] and Keita Ito[1#]

[1]Orthopaedic Biomechanics, Department of Biomedical Engineering, Eindhoven University of Technology, Eindhoven, The Netherlands

[*]Shared first authorship

Roman Dittmar, Ph.D.

Tel: +31 40 247 5169, fax: +31 40 247 3744, r.dittmar@tue.nl

Department of Biomedical Engineering

Eindhoven University of Technology

PO Box 513, GEM-Z 4.13

5600 MB Eindhoven, The Netherlands

Marc M. van Rijsbergen, M.Sc.

Tel: +31 40 247 5675, fax: +31 40 247 3744, m.m.v.rijsbergen@tue.nl

Department of Biomedical Engineering

Eindhoven University of Technology

PO Box 513, GEM-Z 4.09

5600 MB Eindhoven, The Netherlands

[#]Address for correspondence:

Keita Ito, M.D., Sc.D.

Tel: +31 40 247 3851, fax: +31 40 247 3744, k.ito@tue.nl

Department of Biomedical Engineering

Eindhoven University of Technology

PO Box 513, GEM-Z 4.115

5600 MB Eindhoven, The Netherlands

Abstract

Study design: Collagen fiber orientation analysis in moderately degenerated human cadaveric annulus fibrosus (AF) tissue samples.

Objective: Little is known about changes in tissue architecture during early degeneration of intervertebral discs (IVDs). As collagen organization strongly affects disc function, the objective of this study was to quantify the AF collagen orientation and its spatial distribution in moderately degenerated IVDs (Pfirrmann grade III).

Methods: AF tissue samples were dissected from four circumferential (anterior, left/right lateral and posterior) and two radial (outer and inner) locations. Cryo-sections were imaged using Second Harmonic Generation (SHG) microscopy and the collagen fiber orientations per location were determined utilizing a fiber-tracking image analysis algorithm. Also, the proportionality between fibers aligned in the primary direction vs. other oriented fibers was determined

Results: Mean collagen fiber angles ranged between 21° to 31° for outer and 15° to 19° for inner AF samples. Mean collagen orientations at circumferential locations were only significantly different from each other at inner anterior and lateral location. Similarly, fiber angles between the outer and inner AF were not significantly different except at the posterior location. Fiber orientation proportionality did not show large variations. Except for a significant difference in outer AF proportionality between posterior and lateral position, no other differences were observed.

Conclusion: The results of this study provide the first quantitative evidence that the collagen fiber orientation of moderately degenerated discs exhibits a spatially rather homogeneous distribution and typical collagen orientation gradients characterizing healthy IVDs are only partially retained.

Keywords: intervertebral disc; annulus fibrosus; collagen orientation; Second Harmonic Generation

Abbreviations: Intervertebral Disc (IVD), Nucleus Pulposus (NP), Annulus Fibrosus (AF), Outer Annulus Fibrosus (OAF), Inner Annulus Fibrosus (IAF), Second Harmonic Generation (SHG), Matrix Metalloproteinase (MMP), Root Mean Square (RMS), Analysis of Variance (ANOVA).

Introduction

Degeneration of intervertebral discs (IVDs), the pads of fibrocartilage located between the vertebral bodies of the spine, is commonly thought of being a major source of low back pain[1]. This multi-faceted condition involves cell-mediated biochemical and structural changes to both the center of the IVD, the nucleus pulposus (NP), and its surrounding ring of tissue, the annulus fibrosus (AF)[1].

Based on cellular and structural differences, the AF can be further divided into an outer AF (OAF) and an inner AF (IAF)[2]. Measured from the disc periphery, the OAF consists of the first 18 lamellae, whereas the IAF comprises the next 20 lamellae[3]. Within each lamella, collagen fibers are oriented with a distinct mean angle of ± 30° (alternating between lamellae) with respect to the transverse plane of the spine[2,4,5]. As shown by Cassidy et al.[3] and Holzapfel et al.[4], this angle varies with location, both radially and circumferentially, leading to a spatially heterogeneous collagen fiber organization in healthy human AF tissue. Specifically, collagen fiber angle increases radially from ca. 30° in the OAF towards ca. 45° in the IAF[3] and it also increases circumferentially from about 30° at the anterior to ca. 50°[4] at the posterior location This implies that collagen fibers in healthy AF tissue become increasingly oriented in vertical direction towards the NP and at the posterior location.

The unique lamellar collagen organization of the AF is affected during IVD degeneration. As discs degenerate, structural damage and injury occurs including fissures and tears specifically in the AF[6]. Around these severe annular defects, the collagen architecture is remodeled as part of an attempted repair process. Likely, this process is governed by extracellular matrix degrading enzymes, e.g. matrix metalloproteinases (MMPs), as previous studies have found a clear association between MMP expression and tear formation[7]. Furthermore, degenerated discs are

characterized by a less apparent distinction between the NP and the AF due to tissue fibrosis. Consequently, the number of distinct lamellae in the AF decreases, whereas the thickness of the remaining concentric layers increases[2]. Ultimately, in severely degenerated IVDs, such progressive degenerative changes lead to a high annular disorganization of the collagen network[8], i.e. the spatially heterogeneous collagen fiber organization typically observed in healthy AF tissue is lost in severely degenerated discs.

Computational studies have shown that the biomechanical environment of the AF and consequently of the entire disc are dramatically affected when the fiber orientation is altered as local stresses may increase by 100% and total shear strains up to 50%[5,9]. While it is well established that severely degenerated IVDs exhibit a high annular disorganization of their collagen network[8], less is known about (possible) effects of degeneration on the annular collagen fiber architecture of moderately degenerated IVDs. As mechanics directly influences disc cell metabolism[10] and thus cellular function and survival, long-term success of novel regenerative therapies aiming at treating early/mild degeneration will likely also depend on a thorough understanding of the biomechanical environment they are exposed to[11]. Furthermore, potential changes to the AF collagen organization may serve as a biomarker for improved diagnosis of moderate IVD degeneration, where with the advent of novel imaging techniques such as Diffusion Tensor Imaging[12], collagen orientation may potentially be assessed in the clinic.

Hence, the aim of this study was to quantify the AF collagen orientation in moderately degenerated discs (Pfirrmann grade III). Cryosections of AF tissue from human cadaveric discs were obtained and visualized using Second Harmonic Generation (SHG) microscopy. Images were obtained of samples from four circumferential locations (anterior, left lateral, right lateral and posterior) and two different radial locations (OAF and IAF). Using a collagen fiber tracking

algorithm, the primary collagen fiber orientation per location as well as the proportionality between fibers aligned in the primary direction vs. non-primary oriented fibers was determined.

Materials and Methods

Sample preparation

Cadaveric human lumbar spines (L1-S1) were provided by the Anatomy Department of the University Medical Center Utrecht (Utrecht, The Netherlands) following an IRB approved protocol. T2-weighted MRI images of the spines were acquired and all IVDs were graded by a senior radiologist of the Polyclinique Saint-Côme (Compiegne, France) according to the Pfirrmann scale[13]. Only grade III discs were utilized for further analysis. In total, seven IVDs (levels L1-L2 and L3-L4) from five different donors (all male, mean age 62.8 ± 12 years) were dissected by cutting transversally underneath the superior endplate using a scalpel. IVD pieces containing both OAF and IAF were dissected by making vertical incision and cutting transversally above the inferior endplate. For each disc, samples were obtained from the anterior, left and right lateral, and posterior location (Figure 1a). According to Cassidy et al.[3], the OAF consists of the outer 18 lamellae (ca. 2 mm as measured from disc periphery), whereas the IAF comprises the next 20 lamellae (till about 7 mm). Hence, specimens were split into an OAF sample and an IAF sample by cutting the dissected IVD piece at 2 mm from the outside using a razor blade (Figure 1b). Instead, IAF samples were put into molds with their innermost circumferential surfaces tangent to the faces of the molds. Samples were embedded in cryo-glue (Sakura Finetek Europe, The Netherlands) together with three 0.3 mm diameter graphite leads (Pentel, Japan) next to them (Figure 2). These leads were used as markers of each sample when they were taken out of the molds and mounted on the cryotome. After freezing overnight at -30°C,

samples were mounted on a cryotome (Fisher Scientific, The Netherlands) and 50 μm thick tangential cryo-sections of the OAF and IAF were obtained.

SHG microscopy

SHG images of the OAF and IAF cryo-sections were acquired on a Leica TCS SP5X laser scanning microscope (Leica, Germany) with a 10x, 0.4 numerical aperture (NA) objective and excitation light tuned to 810 nm. The SHG signal was collected through a tunable hybrid detector set to 390-420 nm. Tiled scans usually comprising 80 individual SHG images were obtained to cover the entire cryo-section.

Image registration and analysis

SHG images of the acquired tiled scans were stitched into a so-called mosaic image of the entire OAF or IAF cryo-section (Figure 3). As the cryo-sections were rotated with respect to the transverse plane when placing samples into the cryo-molds, the mosaic images had to be first corrected for this rotation prior to further image analysis. Hence, mosaic images were loaded into a custom written Matlab (Matlab, U.S.A) script. First, the vertical edges of the OAF or IAF sample were defined by manually selecting two points, P1 and P2, located on the edge of the sample (Figure 3a). Second, three other points, P3, P4 and P5, located equally distributed between these initial two points and on the edge of the sample, were automatically determined. A line was plotted through P1 and P2, then P3 was defined as a point on the sample edge with y-coordinate equal to the center of the plotted line (Figure 3b). Next, lines through P1 to P3 and P3 to P2 were plotted (Figure 3c). First the center points of the lines through P1 to P3 and P3 to P2 were calculated, respectively. Then the points on the sample edge with y-coordinate equal to the center points were defined as P4 and P5 (Figure 3c). Finally, a line was fitted through all five

points using a linear least squares fitting technique (Figure 3d). The same approach was repeated for the opposite edge of the sample leading to two reference lines with a certain angle with respect to the transverse plane (Figure 3d). A third, final line was calculated by averaging both reference lines (Figure 3d). Mosaic images were rotated until this third, final reference line was aligned in vertical direction (Figure 3e). The first mosaic image, into the depth of the section, containing aligned collagen fibers was used for fiber orientation analysis. A sub-image was manually cropped out of the mosaic image (Figure 3f) and an in-house-developed algorithm[14] was used for quantifying the collagen fiber orientations in the cropped image(s) (Figure 4a). To make sure the outcome of the manually selected sub-image was representative for the entire section, this procedure was repeated at least three times per mosaic image. Care was taken that the sub-images were selected from different locations of the mosaic image (i.e. not taken from the same region).

Based on this algorithm, a histogram was created of each sample and the primary collagen fiber orientation was defined as the angle value with maximum number of counts (Figure 4b). Collagen fiber angles with an angle value of more than 90 degrees represent the same angle value as the angle minus 90 degrees as no presence of head and or tail could be determined. For the purpose of the current study, both values represent the same direction. Therefore, all results will be given as fiber angle between 0 and 90 degrees. To determine the proportionality of the collagen fibers in the primary direction vs. non-primary directions, as measurement of collagen anisotropy, the root mean square (RMS) of the total counted angle values was used to distinguish between the different orientations. Fiber orientations with counts lower than the RMS were classified as oriented in the non-primary directions, whereas angles with counts larger than the RMS were identified as fibers in the primary direction (Figure 4b). This approach was validated

by creating multiple idealized distribution ratios (Gaussian shaped curves) from which the distribution was known and comparing the calculated ratio to the known distribution ratio.

Statistical analysis

To determine differences in fiber primary angles and proportionality between locations blocked two-way analysis of variance (ANOVA; blocked per disc) was performed followed by Fisher's LSD post-hoc tests for pair-wise comparisons between fiber values and proportionality, respectively. All statistical analysis was performed using SPSS 20 (IBM, USA) and statistical significance was assumed for $p<0.05$.

Results

Primary fiber angle - OAF

Mean primary collagen fiber angles in circumferential direction ranged between 21° to 31° for the OAF and exhibited a rather large variance at the posterior position (Table 1). No statistically significant differences were found between the mean primary collagen orientations at the various circumferential locations (Figure 5a). A trend for increasing mean primary angle from anterior to posterior position was observed, since angle values at anterior and lateral locations showed great similarity and were generally smaller than those at the posterior position.

Primary fiber angle – IAF

Mean primary collagen fiber angles in circumferential direction ranged between 15° to 19° for the IAF (Table 1). Significant difference were found between anterior and lateral locations

(p=0.032) (Figure 5b). Mean primary collagen fiber angle values at lateral and posterior locations were very similar and larger as compared to the anterior location.

Primary fiber angle – radial direction

In the radial direction, i.e. from OAF to IAF, fiber angles did not show strong alterations depending on the position. A radial gradient in collagen orientation was observed only at the posterior location where OAF and IAF angles were significantly different from each other (p=0.008) (Figure 6).

Fiber proportionality

In both the OAF and IAF, mean primary fiber proportionality was 70 ± 20% (Table 2). OAF samples showed significantly larger fiber proportionality posteriorly than laterally (p=0.030). No other statistically significant differences in proportionality depending on circumferential locations were observed (Table 2). In contrast, IAF samples showed very similar mean fiber proportionalities for all circumferential locations and no statistically significant differences were observed. Also, in radial direction, no statistically significant differences in collagen fiber proportionality between the OAF and IAF at the various locations were found.

Discussion

The unique heterogeneous collagen organization of healthy IVDs was first described in the reports of Cassidy et al.[3] and Holzapfel et al.[4] They showed that fiber orientation in the human AF is highly organized and follows strong radial and circumferential gradients. Mean fiber angle increases from the OAF towards the IAF and also depends on the circumferential location within

the AF. These established collagen fiber gradients in healthy discs are believed to be essential for proper disc biomechanics and function[9]. While it is well established that severely degenerated IVDs suffer from a high annular disorganization of their collagen network[8] with presumably detrimental effects to disc function[1,9], our results indicate that the unique AF collagen fiber architecture may already be affected in moderately degenerated discs. Pfirrmann grade III discs observed in thus study had a more homogenous AF collagen architecture and only partially retained the collagen orientation gradients typical found in healthy IVDs.

This less organized collagen architecture potentially is also consistent with collagen remodeling and the progressive structural changes observed during degeneration. Such changes include dehydration of the NP, loss of distinction between AF and NP due to tissue fibrosis and in later stages the appearance of AF cracks and fissures[1]. With increasing degeneration these cell-mediated degenerative processes affect the lamellar organization of the AF. As the transition between NP and AF fades away, degenerated discs are reported to have less and thicker lamellae[2]. Also, as the NP becomes dehydrated, disc height and intradiscal pressure decrease causing the lamellae of the inner AF to bulge inwards. This in turn may affect the load distribution to these lamellae, potentially inducing or accelerating the remodeling of the AF collagen architecture in order to cope with the altered biomechanical environment. Hence, decrease of spatial gradients in collagen fiber orientation of moderately degenerated discs may be explained by cell-mediated degenerative processes that affect disc biomechanics and trigger disc cells to remodel the AF collagen architecture.

In general, our measurements of fiber angles showed a variance of up to 15° at the different locations (Figure 5, posterior location) similar to studies of healthy AF tissue[4]. As shown by Boos et al.[15] and Marchand et al.[2], this large variance may be explained by the natural heterogeneity of fiber orientations within the AF and is not related to the utilized imaging or orientation analysis

technique. SHG microscopy has been extensively used to visualize fibrillar collagens and their organization with the resolution and detail of standard histology[17]. Since the orientation of collagen fibers in the acquired SHG images was successfully quantified (Figure 4), this further suggests that the determined large variance is of biological origin, i.e. characteristic of (human) degenerated AF tissue. Our results, obtained on moderately degenerated IVDs, showed a somewhat inhomogeneous variance distribution where the posterior samples showed larger variance than specimens from other locations. This is likely due to more severe morphological changes of degeneration in AF tissue typically found at the posterior position. Posteriorly, IVDs are much thinner and more prone to injury such as herniation[4].

As the large variance may have blurred our results, a power analysis on the obtained angle values was conducted. The calculated power for all comparisons, except for the test between anterior and lateral IAF, was below 80% and, therefore, sample size would have had to be doubled (n = 15) to increase power for all locations (to a minimum of 80%). However, to detect similar differences between the locations as reported for healthy discs, n would also have to be increased and reports of collagen orientations in healthy AF tissue with larger n (n=11) showed similarly large variances[4]. Thus, such large sample sizes are indicative of the observed large variance in collagen fiber orientation of both healthy and moderately degenerated IVDs, and not related to the used imaging, image processing technique or small sample size. This suggests that the observed decreased annular organization of moderately degenerated discs is likely a real effect of tissue remodeling and not an artifact due to measuring too few samples.

Decreased spatial heterogeneity in the collagen architecture during moderate degeneration as shown in this study will have implications on disc mechanical behavior and load-bearing function[4,5]. This in turn may induce more or accelerate degenerative changes in the IVD, as the biomechanical environment is known to directly influence disc cell metabolism[10]. Elaborate

computational models describing healthy IVD mechanics exist that include collagen fiber orientation and in the case of Schroeder et al.[18], also fiber proportionality. As other model parameters such as biochemical content (water, proteoglycans, and collagen) are known for degenerated discs, the results of this study may be incorporated to obtain a computational model of a (moderately) degenerated disc. This would further aid in improving the efficacy of novel regenerative medicine approaches, e.g. cell therapy, aiming at treating early degenerated discs. Since injected cells would be exposed to the same environment that promoted disc degeneration in the first place, a thorough understanding of how altered mechanics due to a more spatially homogenous collagen organization affects disc cell metabolism may increase long-term success of such regenerative approaches[11].

In summary, the results of this study provide the first evidence that moderately degenerated IVDs are characterized by a spatially more homogeneous collagen fiber orientation. Typical collagen fiber gradients characterizing healthy IVDs were only partially retained in moderately degenerated human AF tissue. Hence, quantitative data on how degeneration affects collagen architecture specifically in the AF is obtained. This may lead to a better understanding of the mechano-biological environment of moderately degenerated discs and, thus, key processes and risk factors involved in disc degeneration may be better understood potentially leading to improved therapy. Also, these findings may result in an earlier diagnosis of degenerative changes as a more homogenous fiber architecture may serve as a biomarker for moderate disc degeneration.

Acknowledgements

We thank Prof. Ronald Bleys from the Department of Anatomy Utrecht Medical Center (Utrecht, The Netherlands) for providing cadaveric human lumbar spines and his help with dissecting

samples and Henk de Jong and Dr. Arnold Schilham for x-ray imaging of the lumbar spines. We also acknowledge Prof. Marie Christine Ho Ba Tho, Dr. Tien Tuan Dao, Ludovic Roberta and Dr. Khalil Ben Mansour from Université de Technologie de Compiègne (Compiegne, France) and Dr. Fabrice Charleux from the Polyclinique Saint-Côme (Compiegne, France) for MRI imaging and grading the specimens according to the Pfirrmann scale. The authors would also like to thank Dr. Frans Kanters from the Department of Biomedical Engineering, Eindhoven University of Technology (Eindhoven, The Netherlands) for his valuable assistance with the collagen fiber tracking algorithm.

This research was partially funded by the European Community's Seventh Framework Programme (FP7/2007-2013) under grant agreements MySpine (No. 269909) and Genodisc (201626).

References

1. Urban J P, Roberts S. Degeneration of the intervertebral disc. Arthritis Research & Therapy 2003;5;120-30.

2. Marchand F, Ahmed A M. Investigation of the laminate structure of lumbar disc anulus fibrosus. Spine (Phila Pa 1976) 1990;15;402-10.

3. Cassidy J J, Hiltner A, Baer E. Hierarchical structure of the intervertebral disc. Connective Tissue Research 1989;23;75-88.

4. Holzapfel G A, Schulze-Bauer C A, Feigl G, Regitnig P. Single lamellar mechanics of the human lumbar anulus fibrosus. Biomechanics and Modeling in Mechanobiology 2005;3;125-40.

5. Guerin H A, Elliott D M. Degeneration affects the fiber reorientation of human annulus fibrosus under tensile load. Journal of Biomechanics 2006;39;1410-8.

6. Videman T, Nurminen M. The occurrence of anular tears and their relation to lifetime back pain history: a cadaveric study using barium sulfate discography. Spine (Phila Pa 1976) 2004;29;2668-76.

7. Weiler C, Nerlich A G, Zipperer J, Bachmeier B E, Boos N. 2002 SSE Award Competition in Basic Science: expression of major matrix metalloproteinases is associated with intervertebral disc degradation and resorption. European Spine Journal 2002;11;308-20.

8. Haefeli M, Kalberer F, Saegesser D, Nerlich A G, Boos N, Paesold G. The course of macroscopic degeneration in the human lumbar intervertebral disc. Spine 2006;31;1522-31.

9. Noailly J, Planell J A, Lacroix D. On the collagen criss-cross angles in the annuli fibrosi of lumbar spine finite element models. Biomechanics and Modeling in Mechanobiology 2011;10;203-19.

10. Fernando H N, Czamanski J, Yuan T Y, Gu W, Salahadin A, Huang C Y. Mechanical loading affects the energy metabolism of intervertebral disc cells. Journal of Orthopaedic Research 2011;29;1634-41.

11. Kandel R, Roberts S, Urban J P. Tissue engineering and the intervertebral disc: the challenges. European Spine Journal 2008;17 Suppl 4;480-91.

12. Hsu E W, Setton L A. Diffusion tensor microscopy of the intervertebral disc anulus fibrosus. Magnetic Resonance in Medicine 1999;41;992-9.

13. Pfirrmann C W, Metzdorf A, Zanetti M, Hodler J, Boos N. Magnetic resonance classification of lumbar intervertebral disc degeneration. Spine (Phila Pa 1976) 2001;26;1873-8.

14. Daniels F, Ter Haar Romeny B M, Rubbens M P, van Assen H. Quantification of collagen orientation in 3D engineerd tissue. IFMBE 2006;15;282-5.

15. Boos N, Weissbach S, Rohrbach H, Weiler C, Spratt K F, Nerlich A G. Classification of Age-Related Changes in Lumbar Intervertebral Discs: 2002 Volvo Award in Basic Science. Spine 2002;27;2631-44.

16. Zipfel W R, Williams R M, Christie R, Nikitin A Y, Hyman B T, Webb W W. Live tissue intrinsic emission microscopy using multiphoton-excited native fluorescence and second harmonic generation. Proc Natl Acad Sci U S A 2003;100;7075-80.

17. Schroeder Y, Huyghe J M, van Donkelaar C C, Ito K. A biochemical/biophysical 3D FE intervertebral disc model. Biomech Model Mechanobiol 2010;9;641-50.

Figure 1: Schematic representation of the sample isolation and preparation.

a) Per IVD, 4 wedge-shaped pieces containing both OAF and IAF were dissected. b) After isolation, each IVD piece (posterior sample shown in schematic) was split in an OAF and IAF sample. Dotted lines represent razor blade dissection sites.

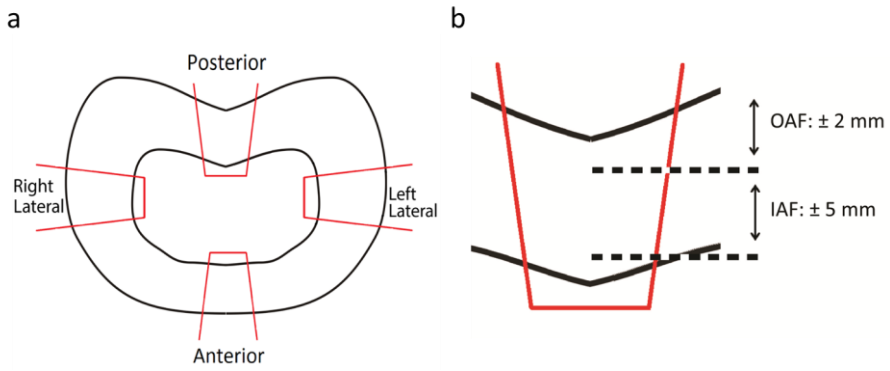

Figure 2: Schematic drawing of sample embedding.

Each isolated OAF and IAF piece was put into a cryo-mold and embedded in cryo-glue. Graphite leads (grey bars) were inserted next to samples.

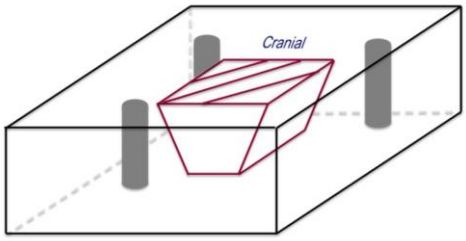

Figure 3: Image registration steps.

a) Representative mosaic image prior to registration. Two points, P1 and P2 are manually selected on sample edge. b) Plotted line through P1 and P2. P3 is automatically determined as

point on the sample edge with y-coordinate equal to the line center. c) P4 and P5 are determined in the same procedure resulting in five equally distributed points on sample edge. d) Steps a)-c) are repeated on opposite sample edge leading to two reference lines. Average of both reference lines is calculated: third reference line. e) Mosaic image is rotated until third reference line is aligned in vertical direction. f) Sub-image is cropped out of aligned mosaic image for collagen fiber orientation and proportionality analysis.

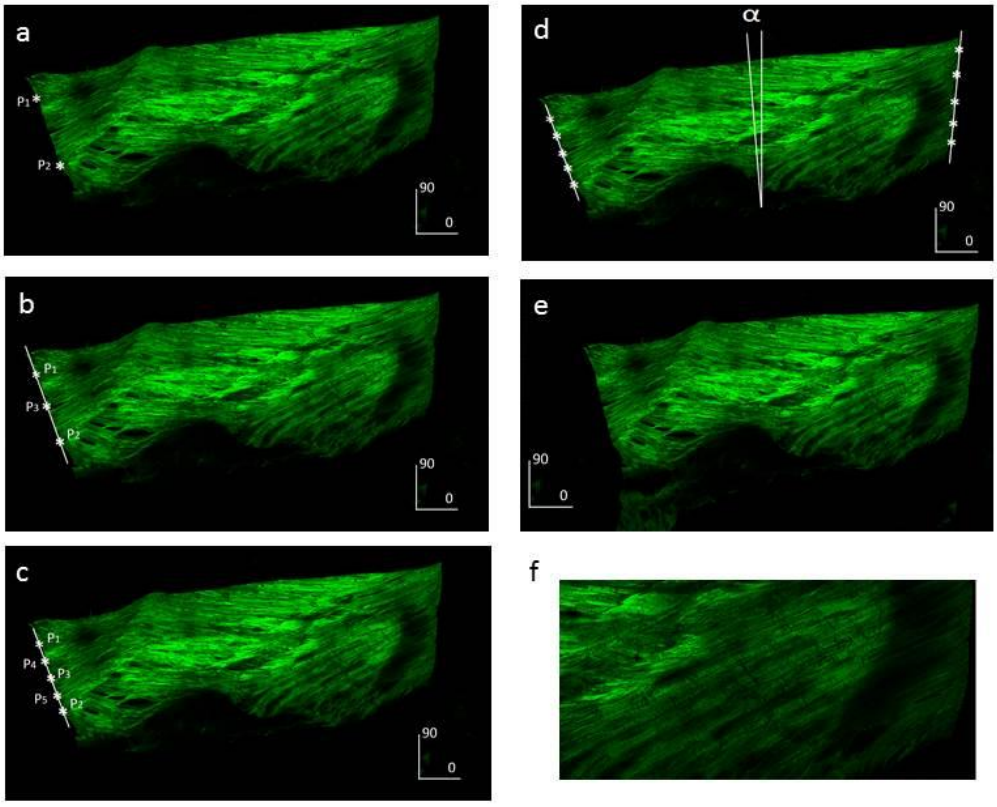

Figure 4: Collagen orientation and fiber proportionality calculation

a) Collagen fiber orientation in cropped sub-image containing aligned collagen. Yellow arrows indicate calculated fiber orientations. b) Corresponding histogram of detected fiber orientations; angle values are with respect to the transverse plane. Red line indicates RMS value used for determining proportionality between fibers aligned in primary direction vs. other directions. Fibers have an angle with a count higher than the RMS value were defined as being in the primary directions, whereas fibers having an angle with a count lower than the RMS value were defined as being in the non-primary directions.

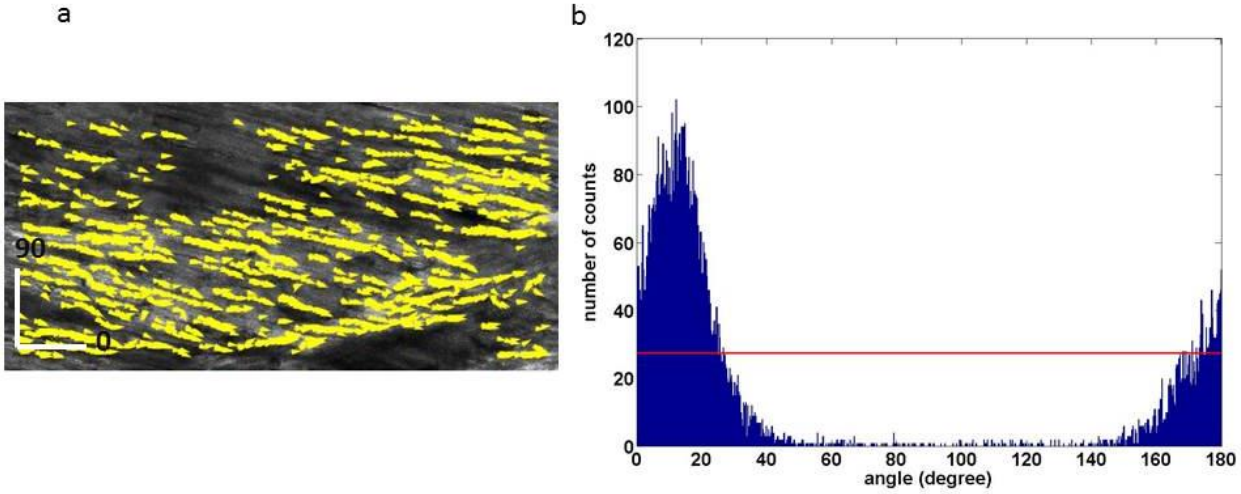

Figure 5: Calculated collagen orientations at various circumferential locations.

Mean primary collagen fiber orientation for OAF (a) and IAF (b) samples at the various circumferential locations. Values are means ± standard deviations (n = 7 for anterior and posterior, n = 14 for lateral).

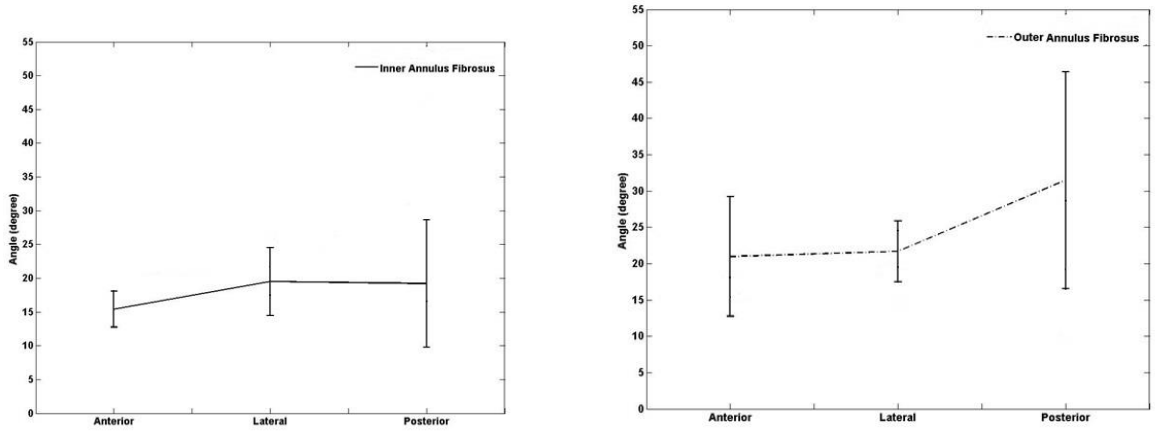

Figure 6: Calculated collagen orientations at various radial locations.

Absolute difference in primary collagen fiber orientation between OAF and IAF at various circumferential locations. Values are means ± standard deviations, including the individual measurements (*; n = 7 for anterior and posterior, n = 14 for lateral). At posterior location, a significant difference in fiber orientation between OAF and IAF was determined (p=0.008,#).

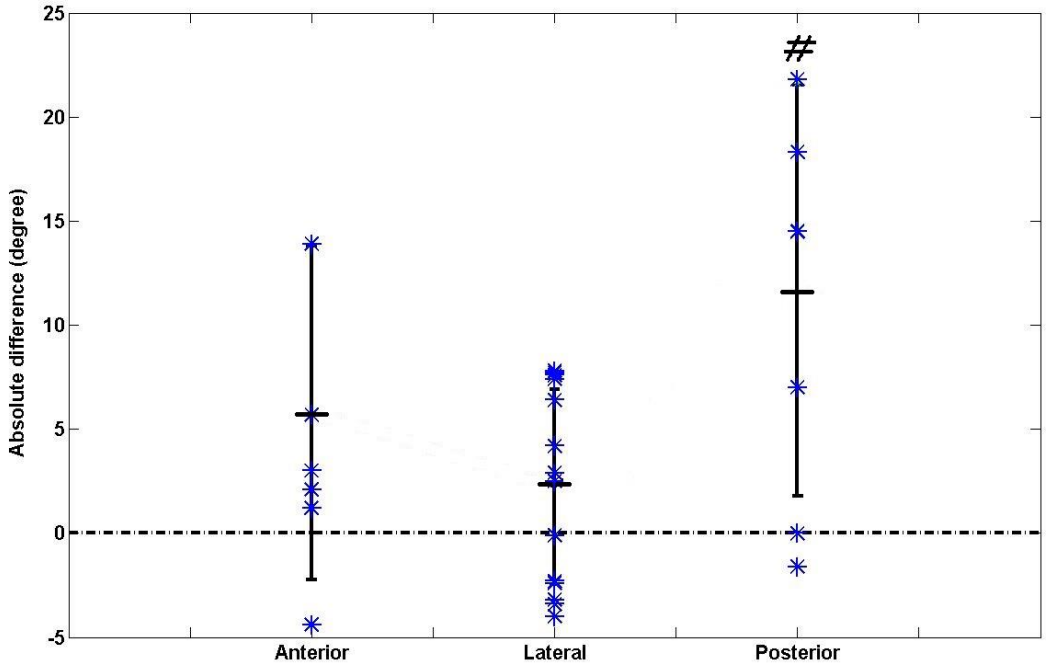

Table 1: Measured collagen fiber proportionality

Measured primary collagen fiber orientation for both OAF and IAF samples at the various circumferential locations. Values are means ± standard deviations (n = 7 for anterior and posterior, n = 14 for lateral).

	OAF (mean ±SD)	IAF (mean ±SD)
Anterior	21.0 ± 8.2°	15.4 ± 2.7°
Lateral	21.7 ± 4.2°	19.5 ± 5.0°
Posterior	31.5 ± 14.9°	19.2 ± 9.4°

Table 2: Measured collagen fiber proportionality

Collagen fiber proportionality (in %) at various circumferential locations. Values are means ± standard deviations (n = 7 for anterior and posterior, n = 14 for lateral). A significant difference between posterior and lateral location of the OAF was found (p=0.030, #).

	OAF (mean ±SD)	IAF (mean ±SD)
Anterior	70 ± 9	72 ± 9
Lateral	66 ± 12$^{\#}$	71 ± 9
Posterior	80 ± 10$^{\#}$	74 ± 12